J. Fluid Mech. (2000), *vol.* 425, *pp.* 187–211. Printed in the United Kingdom

Wave breaking due to internal wave–shear flow resonance over a sloping bottom

By VICTOR I. SHRIRA†, VYACHESLAV V. VORONOVICH‡ AND IGOR A. SAZONOV

Department of Applied Mathematics, University College Cork, Cork, Ireland

(Received 20 January 2000 and in revised form 14 July 2000)

A new mechanism of internal wave breaking in the subsurface ocean layer is considered. The breaking is due to the 'resonant' interaction of shoaling long internal gravity waves with the subsurface shear current occurring in a resonance zone. Provided the wind-induced shear current is oriented onshore, there exists a wide resonance zone, where internal wave celerity is close to the current velocity at the water surface and a particularly strong resonant interaction of shoaling internal waves with the current takes place. A model to describe the coupled dynamics of the current perturbations treated as 'vorticity waves' and internal waves propagating over a sloping bottom is derived by asymptotic methods. The model generalizes the earlier one by Voronovich, Pelinovsky & Shrira (1998) by taking into account the mild bottom slope typical of the oceanic shelf. The focus of the work is upon the effects on wave evolution due to the presence of the bottom slope. If the bottom is flat, the model admits a set of stationary solutions, both periodic and of solitary wave type, their amplitude being limited from above. The limiting waves are sharp crested. Space–time evolution of the waves propagating over a sloping bottom is studied both by the adiabatic Whitham method for comparatively mild slopes and numerically for an arbitrary one. The principal result is that all onshore propagating waves, however small their initial amplitudes are, inevitably reach the limiting amplitude within the resonance zone and break. From the mathematical viewpoint the unique peculiarity of the problem lies in the fact that the wave evolution remains weakly nonlinear up to breaking. To address the situations when the subsurface current becomes strongly turbulent due to particularly intense wind-wave breaking, the effect of turbulent viscosity on the wave evolution is also investigated. The damping due to the turbulence results in a threshold in the initial amplitudes of perturbations: the 'subcritical' perturbations are damped, the 'supercritical' ones inevitably break. As the breaking events occur mainly in the subsurface layer, they may contribute significantly to the mixing and exchange processes at the air/sea interface and in creating significant surface signatures.

1. Introduction

Establishing and understanding the basic mechanisms of mixing in the subsurface layer of lakes and oceans is of interest from many viewpoints. Most physically and

† Present address: Department of Mathematics, Keele University, Keele, ST5 5BG, UK; e-mail:v.i.shrira@keele.ac.uk

‡ On leave from: P. P. Shirshov Institute of Oceanology, Russian Academy of Sciences, 23 Krasikov Str., 117851 Moscow, Russia; e-mail:vvv@wave.sio.rssi.ru.

environmentally important processes, such as energy, gas and heat exchange with the atmosphere, pollutants distribution, phytoplankton life cycles and many others, depend on and often are even directly controlled by the intensity of mixing in the subsurface layer. It is of little wonder that a huge amount of effort has been put into the experimental and theoretical studies of the basic mechanisms determining the intensity and properties of the mixing processes, resulting in a comparatively good, but still insufficient understanding. Direct wind stress, drift currents and their instabilities, tidal currents, both primary and residual (especially important in estuaries and coastal zones), and surface gravity waves breaking are considered to be the most important physical factors contributing to the mixing enhancement.

Yet even the long list above seems to be incomplete. For example, a direct input from internal waves into the mixing processes in the subsurface layer has never been considered to be of importance. Their effect on the sea surface is usually neglected unless the waves are strongly nonlinear or their surface signatures, i.e. wave-induced inhomogeneities of some directly observable factors, such as albedo, sea ice and surface pollutant distribution, surface wave breaking intensity etc., are of interest for their own sake. The reason for this neglect is that the fluid motion induced by the internal wave is usually localized within the thermoclyne well below the surface, and its intensity decreases rapidly upward. However for a particular class of situations the effect of even initially small-amplitude internal waves results in a strongly nonlinear wave motion and breaking events in the subsurface layer. A mechanism for this phenomenon to occur is the direct resonance of the internal waves with the subsurface shear flow. The linear and nonlinear theory of the direct resonance over flat bottom have been developed by Voronovich & Shrira (1996) and Voronovich, Pelinovsky & Shrira (1998, hereinafter referred to as VPS).

The physics underlying this mechanism and the mathematical model to describe it are based on the concept of 'vorticity waves' introduced by Shrira (1989). Suppose that there exists a shear current of boundary-layer type with the velocity monotonically decreasing with the depth, localized in a thin subsurface layer of width h. Within the framework of the inviscid theory, linear perturbations of such a current are composed of singular modes usually referred to as Case waves (Dickey 1960; Case 1960). The remarkable fact which allows one to describe arbitrary flow perturbations within the framework of the wave formalism is that, provided the horizontal scale of the perturbation is much larger than h, an aggregate of the singular Case modes behaves on a certain timescale as if it were a single mode of the discrete spectrum having no singularities in the leading order. These quasi-discrete modes are called 'vorticity waves' as they owe their existence to the inhomogeneous vorticity field provided by the current. They are weakly dispersive, have celerities close to the flow speed at the surface, are very weakly influenced by the stratified fluid below the current's body and can be successfully described within the framework of wave formalism (see e.g. Voronovich, Shrira & Stepanyants 1998).

On the contrary, internal waves are due to the buoyancy forces acting in stratified fluid and in the main order are almost unaffected by the current, provided both their wavelength L and the fluid depth H are large compared to h. Thus, in typical oceanic conditions two physically different types of wave motions may coexist in stratified shear currents, vorticity and internal ones, their influence on each other being generally negligible. However, if the phase speed of a certain internal wave mode is close to that of the vorticity wave mode, a resonance of internal wave and shear flow occurs and a particularly strong interaction takes place. A linear theory of this phenomenon was first proposed by Reutov (1990), who, by employing an asymptotic expansion in

powers of $\epsilon = h/L$, found that the process results in splitting of the mode dispersion curves and $O(\epsilon^{1/2})$ corrections to the wave celerity, instability being present if, and only if, there exist inflection points in the current profile. These results were corroborated by Voronovich & Shrira (1996) who established the interaction to be of the *direct resonance* type, i.e. the vertical structures of the interacting modes have to be close to each other (Akylas & Benney 1980). They also found that the process leads to a significant amplification of the wave motion near the surface: at the resonance conditions the perturbation of the horizontal velocity at the surface proved to be an order of magnitude larger than at the depth, providing an effective mechanism for internal wave surface manifestations.

The next natural step was to develop a nonlinear model. Direct resonances are qualitatively different from, for example, those between internal waves originating from two different thermoclynes. In the latter case only the phase speeds of the modes match, while their vertical structure remains different and a traditional KdV type theory can be applied even at the resonant conditions (see e.g. Gear & Grimshaw 1984). This not being the case for direct resonance, a new theory was required and eventually developed for shallow water with a flat bottom by VPS. The mode amplitudes a and b of the internal and vorticity mode respectively were found to be governed by the system of coupled evolution equations

$$a_t + \Delta a_x - a_{xxx} - b_x = 0, \tag{1.1a}$$

$$b_t + 2bb_x - a_x = 0, \tag{1.1b}$$

where the only parameter Δ is the mismatch in the phase speeds of the interacting waves. The mismatch Δ depends primarily on the water depth and the stratification. A peculiar feature of the interaction is that the internal wave's own nonlinearity does not appear in (1.1), the nonlinear behaviour of the wave being entirely due to the interaction with the vorticity wave. Thus, the resonant mechanism allows even internal waves of comparatively small amplitude to create essentially nonlinear wave patterns in the boundary layer.

From a general viewpoint the system (1.1) is a particular degenerate case of coupled KdV equations. Although the wave dynamics within the framework of the generic coupled KdV system is well known (Grimshaw 2000), this does not help in understanding the particular degenerate case we are interested in. The system (1.1) possesses a rich family of plane steady wave solutions, including solitary waves of two types, moving slightly faster and slower than the linear waves, the amplitude of the 'fast' ones limited from above. The limiting wave is characterized by a sharp corner on the crest. This kind of limiting solution is usually referred to as *peaked solitons* and is very similar to those found in modelling wave breaking within the framework of Whitham's equation (Fornberg & Whitham 1978; Camassa & Holm 1993). Numerical simulations of the initial problem within the framework of (1.1) showed that the solitary waves are 'attractors' for the 'subcritical' localized initial pulses, i.e. with the amplitudes below a certain threshold, while 'supercritical' ones develop vertical slopes at the front in finite time which indicates wave breaking.

One of the major factors greatly influencing and sometimes even controlling the evolution of internal waves on a shelf, the depth variations, was not addressed by VPS for the sake of simplicity. Here we study the evolution of shoaling waves over a sloping bottom in the *resonance zone*. Since the resonant interaction we are studying occurs when the mismatch between the current at the surface and the phase velocity of an internal gravity wave is small (of order of the nonlinearity parameter) and the

celerities of long internal waves vary with the total depth H as $H^{1/2}$, this implies that the depth variation over the resonance zone is necessarily small to ensure the appropriate balance. A rough idea of the possible effect of the depth variations on the waves under consideration can be obtained by comparing stationary wave solutions of (1.1) obtained for different values of constant Δ, which correspond to different fluid depths. The shape of, say, solitary waves depends only on the wave celerity v and the mismatch Δ (see e.g. VPS, figure 4) and varies from very smooth to the limiting peaked solitons. Since Δ changes with the depth, one can expect that, if the wave celerity is fixed in the course of evolution, then any wave should reach the limiting shape as the depth decreases. The reality is more complicated, since, even when the depth variations are adiabatically slow, the celerity does not remain constant, but, nevertheless, this naive argument proves to be robust. In the present work we show that both periodic and solitary shoaling waves inevitably reach their limiting form in finite time. Any further slow evolution is impossible and wave breaking occurs. Direct numerical simulation carried out for arbitrary bottom slope corroborates the analytical results obtained in the adiabatic approximation. Of course, our model does not describe the breaking itself: the equations cease to be applicable in the immediate vicinity of the breaking point.

It is helpful to put the phenomenon we focus on into more general nonlinear wave theory perspective. The internal wave–shear current resonance over a sloping bottom can be viewed as a new example of nonlinear wave transition through a resonant point in an inhomogeneous medium (see e.g. Friedland 1998 and the references cited therein, where different types of such resonances are considered). From this viewpoint this is a common situation, although the equations are new: the wave of one type approaching the resonance point generates or enhances the wave of another type, which for our case means enhancement of the vorticity wave by the internal one. Again, the ways of studying wave nonlinear evolution in a gently inhomogeneous medium up to the point of disintegration are well established and to apply them to a new particular set of equations is relatively straightforward (see e.g. Whitham 1974; Pelinovsky 1996; Agnon, Pelinovsky & Sheremet 1998). The unique peculiarity of the problem under consideration lies in the fact that while wave breaking is usually a strongly nonlinear phenomenon, in our case wave evolution *up to breaking* is adequately described by *weakly nonlinear* equations tractable analytically.

We start § 2 with the derivation of the set of equations governing internal wave–shear flow resonance over a sloping bottom assuming the wave to be long in comparison with the typical total water depth (see figure 1). In the most general formulation the no-flux boundary condition is now formulated at an uneven boundary $z = -H(\boldsymbol{r})$ and separation of variables is impossible even as an approximation, making the problem untractable by analytical means. However, assuming the depth deviation from the mean value in the domain of interest to be small, one can take into account its effect as a perturbation and preserve the asymptotic scheme developed by VPS. Having performed the necessary algebra we arrive at a set of equations similar to (1.1) with only one difference: now the phase mismatch Δ depends on time. In § 3 we study periodic stationary waves occurring within the framework of the original system (1.1) with constant Δ. A complete analysis of even a simplified system with time-dependent phase mismatch is hardly possible at present, though important analytical results can be obtained, if the spatial scale of depth variations is much larger than a typical wavelength. Under this assumption in § 4 we study the adiabatic evolution of the solitary wave solutions of (1.1) with slowly varying Δ, i.e. assume that in each moment T_i the solution is close to the solitary wave of (1.1) with a phase mismatch $\Delta = \Delta(T_i)$.

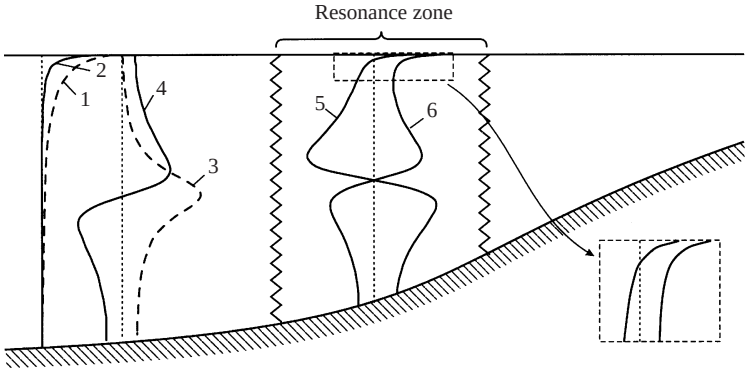

FIGURE 1. Geometry and notation: 1 – unperturbed flow velocity profile $U(z)$; 2 – vorticity mode outside the resonance zone; 3 – Brunt-Väsälä frequency $N(z)$; 4 – internal wave mode outside the resonance zone; 5, 6 – coupled modes. In the right lower corner an expanded view of the region marked by the dashed line is shown.

Such an approach is common for studies of surface and internal wave transformation on a shelf, most often within the framework of KdV or Boussinesq equations with variable coefficients (Grimshaw 1970, 1979; Pelinovsky 1996; Ostrovsky & Pelinovsky 1975; Peregrine & Thomas 1979). The parameters of the solitary wave are supposed to be slowly varying with time and a set of equations governing their evolution on a slower scale is derived. In our study we use Whitham's averaged Lagrangian method (Whitham 1974). The principal conclusion is that all shoaling 'fast' solitary waves inevitably become locally close to the limiting one, i.e. form a singularity at the crest. The solution cannot be continued adiabatically beyond this point and one has the grounds to expect wave breaking to occur. In § 5 we study the evolution of periodic shoaling waves without making any explicit assumptions on the smallness of the bottom slope. A numerical scheme based on the pseudo-spectral methods is applied to trace the evolution of the initial wavelike perturbations. The computations indicate that waves of whatever small initial amplitude do break within the resonance zone. This conclusion is somewhat modified in § 6, where we take into account wave damping to address the situations when the subsurface current becomes strongly turbulent due to particularly intense wind-wave breaking. Then there is a threshold in the initial amplitudes of perturbations: the perturbations below this threshold are dampted, those above inevitably break. The results and some possible implications are briefly discussed in the concluding § 7.

2. Problem statement and asymptotic analysis

As most field observations testify, internal waves in shallow water usually propagate normally to the coastline and are quasi-planar. That is why, as well as for the sake of clarity and simplicity, we hereinafter confine ourselves to the study of planar waves propagating normally to the shore and neglect any variability in the spanwise direction. The starting point is then the standard set of equations (see e.g. LeBlonde & Mysak 1979)

$$u_t + (\boldsymbol{u}\cdot\nabla)u + \frac{p_x}{\rho_0} = 0, \tag{2.1a}$$

$$\mu\,[w_t + (\boldsymbol{u}\cdot\nabla)w] + \frac{p_z}{\rho_0} - b = 0, \tag{2.1b}$$

$$b_t + wN^2 + (\boldsymbol{u}\cdot\nabla)b = 0, \tag{2.1c}$$

$$\nabla\cdot\boldsymbol{u} = 0, \tag{2.1d}$$

where p, b are the pressure and buoyancy perturbations, $\rho_0(z)$ is an equilibrium density distribution and the fluid horizontal velocity $\boldsymbol{u}$ contains both the mean flow and perturbations:

$$\boldsymbol{u} = \boldsymbol{U}(z) + \hat{\boldsymbol{u}}(x, z, t).$$

Equations (2.1) have been made non-dimensional by using a scaling transformation

$$\left.\begin{aligned} &z' = H_0\, z, \quad x' = L\, x, \quad t' = \frac{H_0}{V}\, t, \\ &u' = V\, u, \quad w' = V\frac{H_0}{L} w, \quad N' = \frac{V}{H_0}\, N, \\ &\frac{p'}{\rho_0'} = V^2\frac{p}{\rho_0}, \quad b' = \frac{V^2}{H_0}\, b, \end{aligned}\right\} \tag{2.2}$$

based upon a typical fluid depth H_0, the wavelength L and the basic flow velocity V, with $\mu = \left(H_0/L\right)^2$ being a small parameter corresponding to the weak KdV-type dispersion of internal waves. The boundary conditions are the standard 'rigid lid' at the surface and 'no-flux' at a sloping bottom

$$w\big|_{z=0} = 0, \tag{2.3a}$$

$$uH_x + w = 0 \quad \text{at} \quad z = -H(x). \tag{2.3b}$$

The fluid, thus, is assumed to be composed of two layers: the still core and the subsurface boundary layer containing the shear flow with an effectively different scale of vertical motion. The natural way of treating the problem is to use the smallness of the two parameters describing the wave–flow system, namely μ and $\epsilon = h/H_0$, and to employ the method of matched asymptotic expansions. With that end in view, we first have to find a solution to (2.1) in the core, subject to the no-flux condition (2.3*b*), then to introduce an inner vertical variable in the boundary layer

$$\zeta = \frac{z}{\epsilon} \tag{2.4}$$

and to find an inner solution subject to the 'rigid lid' condition (2.3*a*), and, finally, to match both solutions at $\zeta \to -\infty,\ z \to 0$.

In a standard manner we introduce a set of space–time variables

$$\chi = x - ct, \quad \tau = \mu t, \tag{2.5}$$

corresponding to a perturbation advancing with the celerity c of a resonant long internal wave, with its amplitude evolving on a slower timescale. The analysis of VPS indicates that the dispersive and resonant effects have the same order of magnitude if the balance

$$\epsilon = \frac{h}{H_0} = \mu^2 \tag{2.6}$$

holds. The magnitudes of the motion in the bulk of the fluid and in the boundary layer being quite different, a separate amplitude scaling is required for these two layers.

2.1. *The core solution*

In the core the mean flow is absent and we look for solutions of (2.1), (2.3*b*) in the form of power series of a single small parameter

$$\{u, w, b, p\} = \mu^2 \sum_{n=0}^{\infty} \mu^n \{u_n, w_n, b_n, p_n\}. \tag{2.7}$$

Under condition (2.3*b*) vertical and horizontal variables do not separate and the system is untreatable, unless some additional assumptions on the depth variability are employed. We assume, first, the horizontal scale of the bottom variations to be much larger than the typical wavelength. This implies that the magnitude of bottom variations within the 'resonance zone' is comparatively small, namely

$$H(x) = 1 + \mu\, d(\nu\, x), \tag{2.8}$$

where $\nu \ll 1$ is an additional small parameter which, in principle, may be either smaller or larger than μ. Then the boundary condition (2.3*b*) can be expanded in the Taylor series near the point $z = -1$ and, taking into account the results of the preceeding section, the main-order core solution is just an undisturbed internal wave over the flat bottom:

$$w_0 = -cA_\chi f, \quad u_0 = cAf_z, \tag{2.9}$$

where $A = A(\chi, \tau)$ is the depth-independent amplitude of an internal wave, while $f = f(z)$ is the modal function satisfying the boundary-value problem

$$f_{zz} + \left(\frac{N}{c}\right)^2 f = 0, \tag{2.10a}$$

$$f(0) = f(-1) = 0. \tag{2.10b}$$

The effect of the resonance with the shear flow and the depth inhomogeneity manifests at the next order, as the boundary condition at the bottom is no longer of the rigid lid type. Due to the bottom inhomogeneity the boundary condition at $z = -1$ now reads

$$w_1\big|_{z=-1} = \frac{\partial w_0}{\partial z}\, d, \tag{2.11a}$$

while the presence of the shear flow perturbation changes the boundary condition at $z = 0$. The simplest way to take this effect into account is to require the pressure and streamline displacement to be continuous through the boundary between the flow and the still fluid below, which results in the constraint for vertical velocity

$$w_1\big|_{z=0} = -cB_\chi, \tag{2.11b}$$

with $B = B(\chi, \tau)$ being the amplitude of the vorticity mode in the shear flow layer.

Performing the necessary calculations, finally we find an inhomogeneous boundary problem for w_1, its solution being regular only if a certain compatibility condition is met. Finding this and taking into account (2.11), we obtain an evolution equation for the internal wave amplitude:

$$\alpha A_\tau + \delta A_\chi + \beta A_{\chi\chi\chi} - f_z^{(0)} B_\chi = 0, \tag{2.12}$$

with the superscripts $(0), (-1)$ denoting the values of the variable at $z = 0$, $z = -1$

and the coefficients given by the expressions

$$\alpha = \frac{2}{c}\int_{-1}^{0}\left(\frac{N}{c}\right)^2 f^2 \mathrm{d}z, \quad \beta = \int_{-1}^{0} f^2 \mathrm{d}z, \quad \delta = \left(f_z^{(-1)}\right)^2 d(vx). \tag{2.13}$$

Under the scaling adopted the internal wave's own nonlinearity does not enter (2.12), but due to the coupling with the vorticity wave the former is affected by the nonlinear behaviour of the latter. To close the system of the amplitude equations we have to find the solution in the boundary layer, where the vorticity wave is located, and then to match it with the core solution.

2.2. *The boundary-layer solution*

The vertical scale of motion in the boundary layer is different from that in the core, which means that the relative magnitude of the wave field components specified by (2.7) is no longer valid. However pressure and 'fluid line' displacement, and thus vertical velocity, should be continuous through the boundaries of any fluid layers and this constraint specifies the scaling

$$\{u, w, p\} = \mu^2 \sum_{n=0}^{\infty} \mu^n \{\mu^{-1} u_n, \mu w_n, p_n\}, \tag{2.14}$$

while the buoyancy perturbation as well as the Brunt–Väsälä frequency variation may be neglected. The boundary conditions are rigid lid at the surface $\zeta = 0$ and matching with the core solution at the outer boundary $\zeta \to -\infty$, namely

$$u \to \mu^2 cA + O(\mu^3), \tag{2.15a}$$

$$w \to -\mu^3 cB_\chi + O(\mu^4), \tag{2.15b}$$

$$p \to \mu^2 c^2 A + O(\mu^3). \tag{2.15c}$$

Solving (2.1) and applying the boundary conditions (2.3*a*), (2.15) we find the structure of the vorticity wave in the main order:

$$w_0 = (U - c)B_\chi, \quad u_0 = -U_\zeta B, \tag{2.16}$$

and an evolution equation for the vorticity wave amplitude in the next one:

$$B_\tau - U_\zeta\Big|_{\zeta=0} BB_\chi - \frac{U^2}{U_\zeta}\Big|_{\zeta=0} f_z^{(0)} A_\chi = 0. \tag{2.17}$$

This together with (2.12) forms a closed system of coupled evolution equations governing the dynamics of the internal wave and the shear current perturbations at resonant conditions. Unlike the internal gravity mode the vorticity one is governed by the nonlinear equation (2.17) and so essentially nonlinear wave patterns may result during interaction. According to the scaling used in the bulk of the fluid the disturbance represents mainly the internal wave, whereas in the boundary layer the vorticity mode prevails. This is the principal feature of the phenomenon under consideration and is why the resonant interaction cannot be properly described within the framework of the usual uncoupled models of internal wave evolution. The internal mode itself is indeed weakly influenced by such a 'thin' shear current, i.e. its celerity and mode structure are just slightly disturbed (by an $O(\mu)$ amount). The major effect of the resonance is the excitation of a flow perturbation which is here treated as the vorticity wave and which is much stronger than the initial disturbance.

By means of a scaling transformation

$$\left.\begin{aligned} \Delta &= \left(\frac{U'}{\alpha\left(Uf_z^{(0)}\right)^2}\right)^{1/2}\delta, \quad b = \frac{\left(\alpha U'^3\right)^{1/2}}{2Uf_z^{(0)}}B, \quad a = \frac{\alpha U'}{2f_z^{(0)}}A, \\ t &= \left(\frac{\left(Uf_z^{(0)}\right)^6}{\alpha\beta^2 U'^3}\right)^{1/4}\tau, \quad x = \left(\frac{\alpha\left(Uf_z^{(0)}\right)^2}{\beta^2 U'}\right)^{1/4}\chi, \end{aligned}\right\} \tag{2.18}$$

where all values of the flow velocity and its derivative are taken at the fluid surface, (2.12), (2.17) can be reduced to the non-dimensional form (1.1). It is clear now, that the phase mismatch Δ is directly proportional to the depth variation $d(vx)$. It is useful to transform it to the moving coordinate frame by observing that

$$\Delta(vx) = \Delta(v\chi + v\mu^{-1}c\tau) \simeq \tilde{\Delta}(v\mu^{-1}\tau).$$

The latter approximate equality means that the major effect of the bottom variations is due to the integral change of the depth and not due to variation of the bottom slope.

3. Stationary waves

Clearly, a set of equations with time-dependent coefficients like (1.1) cannot possess any stationary solutions. Yet, if one is interested in the wave dynamics in the system with slowly varying coefficients, these may be of considerable help as was discussed in § 1. So in this section let us assume the bottom to be flat and, hence, Δ to be constant. Under this approximation (1.1) does possess stationary solutions of both periodic and solitary wave type. The latter were studied extensively by VPS, so the primary concern here will be the periodic ones.

Let us look for stationary solutions of (1.1) describing a general wavelike perturbation advancing without change of form with a constant speed:

$$a = a_s(x - vt), \quad b = b_s(x - vt). \tag{3.1}$$

Substituting (3.1) into (1.1) and integrating once with respect to the running variable $\Theta = x - vt$ results in a set of two ordinary differential equations:

$$\frac{\mathrm{d}^2 a}{\mathrm{d}\Theta^2} + (\Delta - v)a + R = b, \tag{3.2a}$$

$$b^2 - vb + P = a, \tag{3.2b}$$

where R and P are constants of integration. They implicitly determine important physical parameters of the periodic wave such as the period, the amplitude and the mean value over the period, subscripts being omitted for brevity. Excluding $a(\Theta)$ from (3.2a) and integrating it once again we get an equation corresponding to the energy equation for a particle in a potential well, Θ being the time and b the coordinate of the particle:

$$\left(\frac{\mathrm{d}b}{\mathrm{d}\Theta}\right)^2 = \frac{1}{(v - 2b)^2}((v - \Delta)\left(b^2 - vb - P\right)^2 - R\left(b^2 - vb + P\right) + \tfrac{4}{3}b^3 - vb^2 - 2Q), \tag{3.3}$$

where Q is an additional constant of integration. For solitary waves having zero

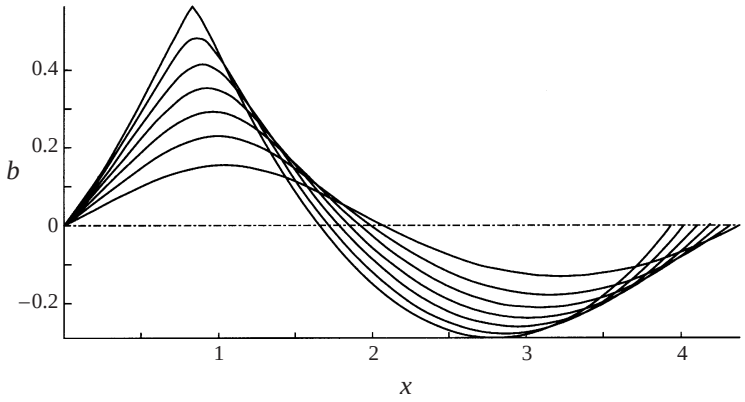

FIGURE 2. Periodic stationary wave solutions of (3.6) ($\Delta = 1.0$, $v = 1.2$).

asymptotics at infinity, all constants of integration are zero and (3.3) coincides exactly with (4.4*b*) of VPS. A straightforward analysis (see VPS for details) indicates that the original set (1.1) possesses two families of solitary waves with speeds in the ranges

$$v \in (c_-; \min\{\Delta, 0\}) \quad \text{and} \quad v \in (c_+; v_+), \tag{3.4a}$$

where the borders of the regions of existence are given by

$$c_\pm = \tfrac{1}{2}\left[\Delta \pm \left(4 + \Delta^2\right)^{1/2}\right], \quad v_+ = \tfrac{1}{2}\left[\Delta + \left(\tfrac{16}{3} + \Delta^2\right)^{1/2}\right]. \tag{3.4b}$$

Waves advancing with the maximal speed v_+ have a singularity, a sharp corner at the crest, and are close to those found by Fornberg & Whitham (1978) in their studies of breaking of surface gravity waves.

Focusing on the studies of periodic waves it is convenient, first, to change the evolutional variable and to rewrite (3.3) in terms of the wave phase $\theta = k\Theta$ by implicitly introducing the wavevector k. Second, for the sake of maximal clarity and simplicity of the final results we confine ourselves to the study of periodic stationary waves having zero mean over the period

$$\{\langle a\rangle, \langle b\rangle\} = \frac{1}{2\pi}\int_{-\pi}^{\pi} \{a, b\}\, \mathrm{d}\theta = 0, \tag{3.5}$$

as constant pedestals can be removed by means of a simple transformation of b, v and Δ. Then averaging (3.2*a*) over the period we find $R = 0$ and, hence, for waves with zero mean, (3.3) takes the much more simple form

$$k^2(b')^2 = \frac{1}{(v-2b)^2}\left((v-\Delta)(b^2 - vb - P)^2 + \tfrac{4}{3}\,b^3 - vb^2 - 2Q\right). \tag{3.6}$$

Provided all roots of the nonlinear potential (the expression on the right-hand side of (3.6)) are real and known, the solution for the periodic wave can be found in closed form in terms of incomplete elliptic integrals of the first and the third kind. Yet that is not of much practical use for analytic calculations as the roots of the fourth-order polynomial can, in general, be found only with the help of numerical methods. To give an idea of how the steady periodic wave solutions look several examples of such solutions of the form ranging from quasi-linear to the limiting one constructed numerically are depicted in figure 2.

Nonetheless, one is able to proceed with analytical methods if any two of the four

roots of the nonlinear potential are close to each other. One of these cases corresponds to solitary wave solutions and was thoroughly studied by VPS, another corresponds to small-amplitude periodic waves asymptotically close to linear ones, while in the third case the solution is close to the limiting periodic wave.

3.1. *Small-amplitude waves*

In this subsection, we are interested in small-amplitude waves, close to the harmonic solutions of (3.6) and having zero mean over the period. This implies, first, that the motion of the imaginary particle occurs in the immediate vicinity of the point $b = 0$ and, second, that the values of the constants are of order of the wave amplitude squared. Therefore we expand the right-hand side of (3.6) into Taylor series in b and introduce a new constant

$$q = Q - \tfrac{1}{4}(v - \Delta)\left(v^2 P + 2P^2\right), \tag{3.7}$$

This procedure results in the simplified equation for small-amplitude waves

$$k^2 \left(b'\right)^2 = \tfrac{1}{2}(v - \Delta)P - 2\,\frac{q}{v^2} - 8\,\frac{q}{v^3}\,u - \beta^2 b^2 - \alpha^2 b^3, \tag{3.8a}$$

with the coefficients being positive and given in explicit form by the expressions

$$\beta^2 = \frac{1 + v\Delta - v^2}{v}, \quad \alpha^2 = 2\,\frac{\frac{4}{3} + v\Delta - v^2}{v^2}. \tag{3.8b}$$

Note that the terms of order higher than u^3 are omitted as well as small (an order of q) corrections to α^2, β^2, as our primary interest at this stage is in linear waves and the first nonlinear corrections to them.

The solution to (3.8) is sought in the form of an non-harmonic wave of small amplitude ($\varepsilon \ll 1$) having zero mean over a period:

$$b = \varepsilon\, b_1 \cos(\theta) + \varepsilon^2 b_2 \cos 2\theta + \cdots. \tag{3.9}$$

On substituting (3.9) into (3.8) and equating main-order coefficients occurring in zero to third harmonics, we find the dispersion relation for linear waves in the implicit from

$$k^2 = \frac{1 + v\Delta - v^2}{v}, \tag{3.10}$$

and the constants P, q (and, hence, Q) and the amplitude of the second harmonic, which are related to the first-harmonic amplitude by the expressions

$$P = -\varepsilon^2\,\frac{b_1^2}{2}, \tag{3.11a}$$

$$q = \varepsilon^2\,\frac{3v}{8}\,\left(v^2 + v\Delta - \tfrac{4}{3}\right)\,b_1^2 \quad \Rightarrow \quad Q = \varepsilon^2\,\frac{v}{2}\,\left(v^2 - v\Delta - 1\right)b_1^2, \tag{3.11b}$$

$$b_2 = \frac{1}{2v}\,\frac{v^2 - v\Delta - \frac{4}{3}}{v^2 - v\Delta - 1}\,b_1^2. \tag{3.11c}$$

It is easy to show that the dispersion relation (3.10) coinsides exactly with (4.2) of VPS found by direct linearization of (1.1) and therefore the regions of linear wave existence in Fourier space are determined by

$$v \in (-\infty; c_-) \quad \text{and} \quad v \in (0; c_+), \tag{3.12}$$

the borders given by (3.4*b*).

3.2. *Limiting waves*

Another important solution which can be obtained by analytical means is the limiting wave. Like their solitary counterparts the limiting periodic waves exist only in the 'fast' wave family, i.e. moving faster than the linear one ($v > \Delta$). As shown below, if two larger roots of (3.6) coincide, this always occurs at the value $b_+ = v/2$ at which the singularity in the potential takes place. This singularity of the double-pole type is the reason for limiting wave appearance. It results from the simple fact that the fluid particles in the wave cannot move faster than the wave itself (the multiplyer $1/2$ is due to a specific form of non-dimensionalization employed in (1.1)). To obtain a better insight into the problem, first note that the roots of (3.6) coincide with the roots of its numerator

$$\mathscr{S} = (v-\Delta)\left(b^2 - vb + P\right)^2 + \tfrac{4}{3}b^3 - vb^2 - 2Q \tag{3.13}$$

and therefore its double roots occur at the points which are simultaneously zeros of its first derivative

$$\mathscr{S}' = -2(v-\Delta)(v-2b)\left(b^2 - \frac{v^2 - v\Delta - 1}{v-\Delta}\,b + P\right). \tag{3.14}$$

From (3.14) it is clear that one of the extrema, which we are interested in, does occur at $b = v/2$, the point of the singularity in the potential. The condition of this point to be simultaneously a zero of (3.13) imposes a constraint on the possible values of wave parameters, i.e. for a limiting wave an equality

$$Q = \tfrac{1}{2}(v-\Delta)P^2 - \frac{v^2}{4}(v-\Delta)P + \frac{v^3}{32}\left(v^2 - v\Delta - \tfrac{4}{3}\right) \tag{3.15}$$

must hold. In the case of solitary waves, i.e. at $P = Q = 0$, (3.15) yields the value of the limiting wave speed v_+ given by (3.4*b*).

Taking into account (3.14) and (3.15) it is helpful to make the mapping $w = b - v/2$ which results in a significantly simplified form of (3.6):

$$k^2\left(w'\right)^2 = (v-\Delta)w^2 + \tfrac{4}{3}w + 2(v-\Delta)P - \tfrac{1}{2}v\left(v^2 - v\Delta - 2\right), \tag{3.16}$$

which is valid only for limiting waves. As the crest of the limiting wave with the sharp corner corresponds to $w = 0$, it is simple to find the value of the angle, which is just

$$\tan\frac{\alpha}{2} = \frac{1}{w'(0)} = \frac{2k}{\left[4(v-\Delta)P - v\left(v^2 - v\Delta - 2\right)\right]^{1/2}}. \tag{3.17}$$

Unfortunately, the value of k itself depends on the values of P and v, and this dependence is not very simple (see (3.19) below).

Equation (3.16) can be integrated directly to yield the limiting wave solution in the closed form

$$\mathscr{F}\exp\left(k(v-\Delta)^{1/2}|\theta|\right) = (v-\Delta)^{1/2}\left(w + \frac{2}{3(v-\Delta)}\right) + \left((v-\Delta)(w^2 + 2P) + \tfrac{4}{3}w + \tfrac{1}{2}v\left(v^2 - v\Delta - 1\right)\right)^{1/2}, \tag{3.18}$$

the constant $\mathscr{F}$ to be defined by the initial conditions. To find the value of the wavevector which in this formulation is completely determined by the chosen values

of P, v, Δ one has to integrate over half a period. The result is

$$k = \frac{1}{\pi}(v-\Delta)^{1/2} \ln\left(\frac{2\sqrt{2}/3 + (v-\Delta)^{1/2}\left[v\left(v^2 - v\Delta - 2\right) - 4(v-\Delta)P\right]^{1/2}}{\left[\left(v^2 - v\Delta - \frac{4}{3}\right)\left(v^2 - v\Delta - \frac{2}{3}\right) - 4(v-\Delta)^2 P\right]^{1/2}} \right). \quad (3.19)$$

An example of the limiting wave is presented in figure 2.

4. Evolution and breaking of a shoaling wave: mild bottom slope

Having established the basic features of the internal wave resonant interaction with the shear current over a flat bottom, in this section we take into account the presence of the bottom slope and consider the effect of the bottom variability on the solutions of (1.1). The nature of the process and particular results depend on the relation between the parameter ν, appearing in (2.8), and μ, i.e. on the scale of bottom variability λ as compared with other spatial scales of the problem. The flat-bottom problem is characterized, basically, by two horizontal scales: the wavelength, which is unity in our scaling, and the spatial scale of the wave amplitude evolution L_e, which is of order $\mu^{-1}L$. If $\lambda \sim L_e$ the phase mismatch depends on the same timescale as the wave field components and the original system (1.1) with variable coefficients does not seem to be treatable by analytical means. Some approximate solutions can be found just in two limiting cases. If the bottom in the domain of resonance is 'steep', so that $\lambda \ll L_e$, one can approximate it by a step function and study the problem of a wave passage over it, matching the solutions in two regions of the flat bottom by means of some conservation laws derived from the original equations. In the opposite limit, $\lambda \gg L_e$ and, thus, $\nu \ll \mu$, one can look for solutions in terms of adiabatic perturbations, with the main-order term being locally a stationary wave over a flat bottom, the parameters of which vary slowly in space and time. Then, a compatibility condition ensuring regularity of the first-order correction results in a set of equations governing the parameters evolution on slower space–time scales.

4.1. *Averaged variational principle*

Here we focus on the second problem as the most relevant for the description of internal wave transformation and breaking in the shelf zone. The most convenient way to study it is to apply Whitham's method based on the Lagrangian formulation of the original problem, which was developed originally for periodic wavetrains (Whitham 1965) and successfully applied later to solitary waves as well (Grimshaw 1970; Pelinovsky 1996). Briefly, this procedure consists of calculating the average value of the Lagrangian density over one period for the uniform wavetrain, which itself depends on a set of parameters such as frequency, wavevector, mode amplitudes, etc. The average Lagrangian is then subjected to variations with respect to these parameters, which leads to the so-called transport equations. Equations (1.1) may be considered as a consequence of a variational principle

$$\delta \int \hat{L}\, \mathrm{d}x\, \mathrm{d}t = 0, \quad (4.1a)$$

with the Lagrangian density $\hat{L}$ expressed through the field potentials E, F so that

$$a = E_x, \quad b = F_x, \quad (4.1b)$$

$$\hat{L} = -\tfrac{1}{2}(E_x E_t + F_x F_t) - \tfrac{1}{3}F_x^3 - \tfrac{1}{2}\Delta E_x^2 + \tfrac{1}{2}E_{xx}^2 + E_x F_x. \quad (4.1c)$$

The main-order solutions to (1.1) are now sought in the most general form of a periodic wavetrain on a pedestal, which depends only on the slow variables $T = \beta t$ and $X = \beta x$, $\beta = L_e/\lambda = \nu/\mu$ being the ratio of the nonlinear to the bottom-variability space scales. These variables and the pedestals are treated as constants when averaging over a wave period is carried out. Let

$$a = \mathscr{A} + e(\theta), \quad b = \mathscr{B} + u(\theta), \tag{4.2}$$

where $\theta = k(x - vt)$ is the wave phase and the periodic parts are supposed to have zero mean over the period. The latter can be found in closed form by the same procedure as applied in § 3, the only principal difference being the explicit appearance of the pedestal $\mathscr{B}$ in the analogue of (3.6):

$$k^2(u')^2 = \frac{1}{(v - 2\mathscr{B} - u)^2}((v-\Delta)\left(u^2 - (v - 2\mathscr{B})u + P\right)^2 + \tfrac{4}{3}u^3 - (v-2\mathscr{B})u^2 - 2Q), \tag{4.3}$$

which implicitly determines the dependence of the wave solution on P, Q and $\mathscr{B}$.

Next the Lagrangian should be expressed in terms of the potentials taken in the most general form

$$E = \phi(x,t) + f(\theta), \tag{4.4a}$$

$$F = \psi(x,t) + g(\theta), \tag{4.4b}$$

where

$$\{f, g\} = k^{-1}\int_0^\theta \{e, u\}\mathrm{d}\theta \tag{4.4c}$$

and $\phi = \mathscr{A}x - \mathscr{C}t, \psi = \mathscr{B}x - \mathscr{D}t$ are the so-called 'pseudophases', and then averaged over the period taking into account (3.5). The result is the required averaged Lagrangian

$$\mathscr{L} = \left[\tfrac{1}{2}\left(\mathscr{A}\mathscr{C} - \mathscr{B}\mathscr{D} - \Delta\mathscr{A}^2\right) + \mathscr{A}\mathscr{B} - \tfrac{1}{3}\mathscr{B}^3 + Q\right] + k\mathscr{W}. \tag{4.5}$$

It consists of the mean part in square brackets and the wave part $k\mathscr{W}$. The former depends only on pedestals, while the latter results from averaging over the wave period of the function (3.13) which now takes the form

$$\mathscr{S} = (v - \Delta)\left(u^2 - (v - 2\mathscr{B})u + P\right)^2 + \tfrac{4}{3}u^3 - (v - 2\mathscr{B})u^2 - 2Q, \tag{4.6a}$$

$$\mathscr{W} = \frac{1}{\pi}\oint |v - 2\mathscr{B} - 2u|S^{1/2}\,\mathrm{d}u. \tag{4.6b}$$

If the polynomial $\mathscr{S}(u)$ has the four real roots $u_0 < u_1 < u_2 < u_3$, we select that solution of (3.13) for which u is confined between u_1 and u_2, given $v - \Delta > 0$, and between u_2 and u_3 otherwise, so that the integral in (4.6*b*) is computed over half a period of the wave.

The average Lagrangian $\mathscr{L}$ is a function of eight variables: $\mathscr{A}$, $\mathscr{B}$, $\mathscr{C}$, $\mathscr{D}$, P, Q, ω $(= kv$, the wave frequency) and k. For a slowly varying wavetrain these parameters are functions of X, T and Whitham's procedure is to subject the averaged Lagrangian to variations with respect to constants of integration, 'true' phase θ and pseudophases ϕ, ψ which together with three consistency relations

$$\mathscr{A}_T + \mathscr{C}_X = 0, \tag{4.7a}$$

$$\mathscr{B}_T + \mathscr{D}_X = 0, \tag{4.7b}$$

$$k_T + (kv)_X = 0 \tag{4.7c}$$

form a set of eight equations governing the dynamics of the wavetrain. These equations describe slow space–time changes of its amplitude, celerity and period as well as of the pedestals. Performing the necessary calculations we arrive at the set

$$\delta\phi: \qquad \left(\frac{\partial \mathscr{L}}{\partial \mathscr{C}}\right)_T - \left(\frac{\partial \mathscr{L}}{\partial \mathscr{A}}\right)_X = 0, \tag{4.8a}$$

$$\delta\psi: \qquad \left(\frac{\partial \mathscr{L}}{\partial \mathscr{D}}\right)_T - \left(\frac{\partial \mathscr{L}}{\partial \mathscr{B}}\right)_X = 0, \tag{4.8b}$$

$$\delta\theta: \qquad \left(\frac{\partial \mathscr{L}}{\partial \omega}\right)_T - \left(\frac{\partial \mathscr{L}}{\partial k}\right)_X = 0, \tag{4.8c}$$

$$\frac{\partial \mathscr{L}}{\partial P} = 0, \quad \frac{\partial \mathscr{L}}{\partial Q} = 0. \tag{4.8d,e}$$

This system can be simplified significantly by taking into account the explicit expressions for the averaged Lagrangian and relations between the wave field components. First, it is easy to see that (4.8*d*) results just in the identity $\langle e\rangle = 0$, which is exactly our *a priori* requirement for the wave to have zero mean. Furthermore, (4.8*e*) results in a dispersion relation which determines the inverse wavenumber as a function of other parameters:

$$k^{-1} = -\frac{\partial \mathscr{W}}{\partial Q} = \frac{1}{\pi}\oint |v - 2\mathscr{B} - 2u|\mathscr{S}^{-1/2}\mathrm{d}u. \tag{4.9}$$

Next, (4.8*a*), (4.8*b*) combined with the consistency relations for pseudophases yield transport equations for the pedestals:

$$\mathscr{A}_T + \Delta\mathscr{A}_X - \mathscr{B}_X = 0, \tag{4.10a}$$

$$\mathscr{B}_T + 3\mathscr{B}\mathscr{B}_X - \mathscr{A}_X = \left(k\frac{\partial \mathscr{W}}{\partial \mathscr{B}}\right)_X, \tag{4.10b}$$

which can be easily recognized as the result of substitution of wave field components in the form (4.2) into the original set (1.1) and averaging over the period. Note that the right-hand side of the second equation is just $-\langle u^2\rangle_X$ and thus this term describes the generation of the mean or 'rectified' motion by the nonlinear wave field similar to Reynolds stresses in turbulence theory and to the so-called 'Miller force' in plasma hydrodynamics.

Finally, we note that $\mathscr{W}$ does not depend on ω and k separately but only on their combination $v = \omega/k$, and transform (4.8*c*) into the following form:

$$\left(\frac{\partial \mathscr{W}}{\partial v}\right)_T + \left(v\frac{\partial \mathscr{W}}{\partial v}\right)_X = \frac{\partial \mathscr{W}}{\partial X}, \tag{4.11}$$

where the last derivative should be taken while keeping $v = \text{const}$. The physical meaning of (4.11) can be easily understood if one computes the correspondent derivatives of the function $\mathscr{W}$ and observes that

$$\frac{\partial \mathscr{W}}{\partial v} = \frac{1}{2}\frac{\langle e^2 + u^2\rangle}{k}. \tag{4.12}$$

Thus (4.11) is just the conservation law for the averaged wave action, the reasons for its variation being the bottom slope, the pedestals or the wavevector inhomogeneity in space. The difference between (4.11) and the wave action conservation equation

obtained within the framework of traditional theories (see e.g. Bretherton & Garrett 1968; Whitham 1974) is due to a specific dependence of the depth, and hence the phase mismatch on the space–time variables. Traditionally the environment is supposed to be stationary, but variable in space, whereas the coefficients of (1.1) do not depend on the space variables, but change with time. Therefore, traditionally the wavevector and the wave action E/ω are conserved, while the energy E and the wave frequency ω change as separate variables. Within the framework of our model the wave frequency and the wave action E/k are conserved, if the reflections from the bottom and the tail generation process are neglected. It is worth noting that the conserved quantity E/k acts as wave action in our specific variables only; if we turn back to the primitive physical variables the quantity E/k is still conserved but it acquires a different physical interpretation.

4.2. *Solution of the transport equations*

Finally we have obtained a system which consists of two transport equations for pedestals (4.10), (4.11) for the wave action, the consistency relation for the real phase and two integral constraints: requirement of the wave to have zero mean and the dispersion relation (4.9). For periodic wavetrains wavevector k is of order unity and the equations are strongly interdependent: nonlinear action of the wave field results in pedestal generation which in turn greatly influences wave evolution. However, the system can be considerably simplified if we confine ourselves to studying localized solutions, i.e. solitary waves. Applying Whitham's method, though based on averaging over the period and usually applied to periodic wavetrains, to aperiodic solutions can be successfully justified by the following argument.

Suppose that the constants of integration P, Q tend to zero. The periodic nonlinear wave then becomes asymptotically close to a periodic set of solitary waves. The period, or the distance between the wave humps, as rigorous calculations indicate, becomes asymptotically large in the limit $P, Q \to 0$, its dependence on the constants being described approximately by the expression

$$\frac{2\pi}{k} = \left(\frac{v}{v^2 - v\Delta - 1}\right)^{1/2} \ln\left(2Q + P^2 \frac{v^2 - v\Delta - 1}{v - \Delta}\right)^{-1} + O(\ln\ln P^{-1}). \tag{4.13}$$

One can easily recognize in the first multiplier the inverse value of κ^{-1} (see VPS (4.8)) which is just the typical spatial size of a solitary wave. If the period is so large that its variations can be neglected, the difference between a set of solitary waves and an isolated free solitary wave is asymptotically small. Then Whitham's theory which is valid for a set of solitary waves can also be used for a single solitary wave with an asymptotically small error. Mathematically this means that we can use the derived equations, putting $P = Q = 0$ in the calculations and introducing a formal averaging over a solitary wave as follows:

$$\langle(\ )\rangle = \frac{1}{2\pi}\int_{-\pi}^{\pi}(\ )\,\mathrm{d}\theta \to \frac{k}{2\pi}\int_{-\infty}^{\infty}(\ )\,\mathrm{d}\Theta \to \gamma\left(\frac{v^2 - v\Delta - 1}{v}\right)^{1/2}\int_{-\infty}^{\infty}(\ )\,\mathrm{d}\Theta, \tag{4.14}$$

where $\gamma \sim 1/\ln|Q|^{-1}$ is considered as a small constant parameter and thus can be excluded from (4.11).

One important consequence is that the effect of a solitary wave on the mean motion is asymptotically small (e.g. $\langle u^2\rangle \sim \gamma$), i.e. the right-hand side of (4.10) can be neglected. Then the evolution of pedestals and of solitary wave are decoupled and we can confine ourselves to the study of the case $\mathscr{A} = \mathscr{B} = 0$ (if the pedestals were zero

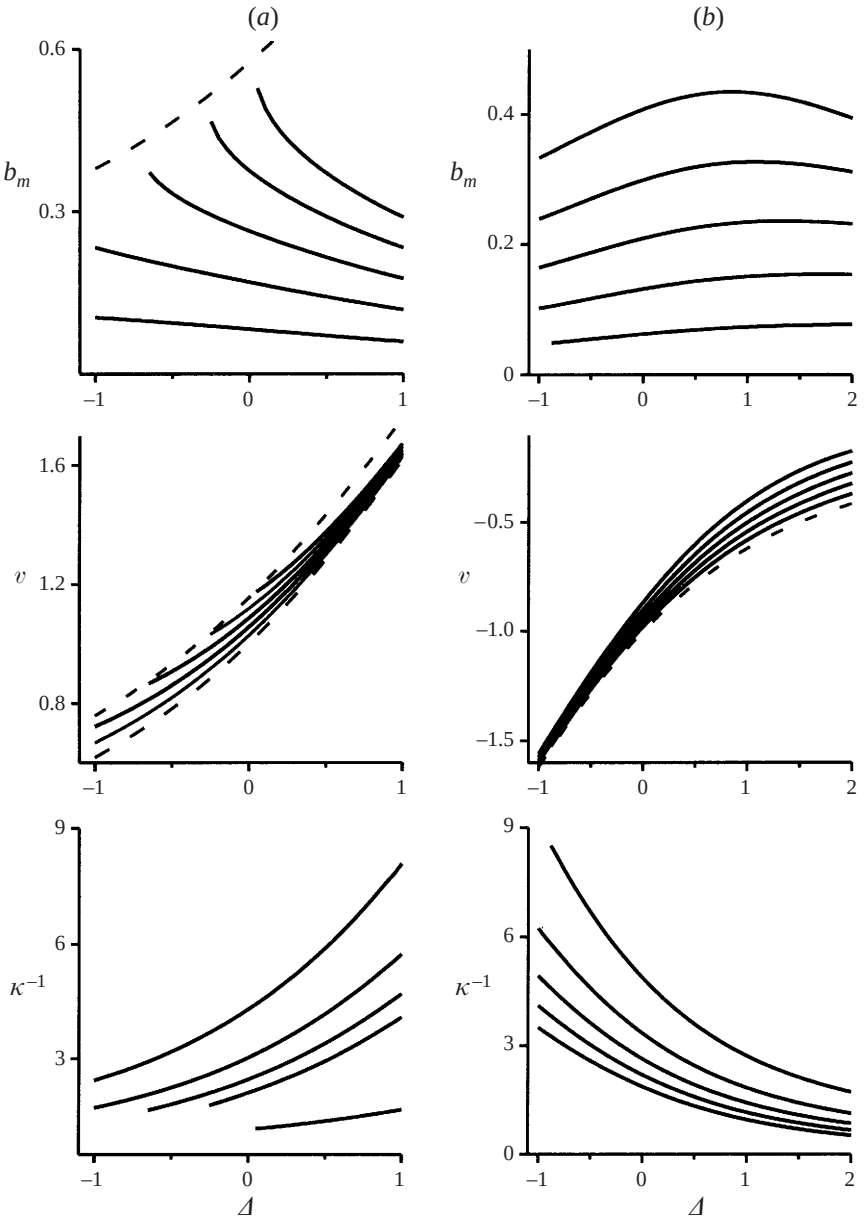

FIGURE 3. Transformation of shoaling solitary waves: (*a*) 'fast'; (*b*) 'slow'. Bold lines trace the adiabatic evolution of the soliton amplitude b_m, velocity v and spatial size κ^{-1} as functions of the mismatch (depth) for different initial conditions. Dashed curves bound the regions of solitary wave existence.

initially they would not be generated in the process of transformation). Thus the only equation remaining to be solved is (4.11). The latter can be simplified even further, as $P, \mathscr{B}$ are now set to zero and the wave action $\mathscr{W}$ depends just on the solitary wave velocity v and an external parameter Δ which is related with the depth variations and is a function of time only. Hence, solitary wave variations in space can also be

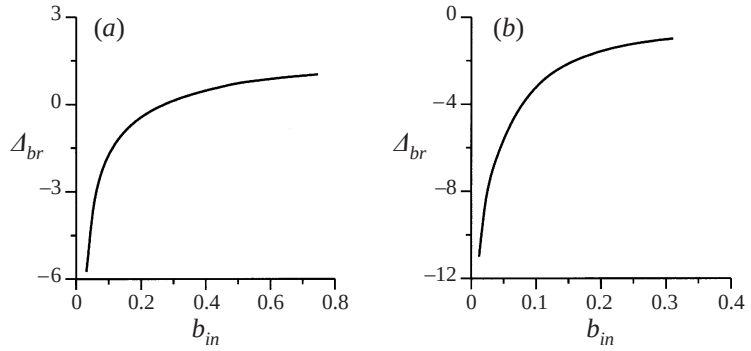

FIGURE 4. Dependence of the critical value of phase mismatch Δ_{br} on the initial wave amplitude b_{in}: the initial value of Δ is set to 1 in (a) and -1 in (b).

neglected and the solitary wave parameters are governed by the very simple equation

$$\frac{\partial \mathscr{W}}{\partial v} = \text{const}, \tag{4.15}$$

which is just the law of conservation of action.

Unfortunately, even from this simplest form it is not possible to derive an explicit analytical law connecting the wave amplitude and the local fluid depth similar to the nonlinear Green's law easily obtained in KdV type theories (Pelinovsky 1996). However, it is straightforward to trace numerically the dependence of the wave amplitude on varying Δ, where the latter is a known function of the depth. The results of such calculations for 'fast' and 'slow' solitary waves are shown in figure 3(a, b) as a family of solid curves in the (v, Δ)-, (u_m, Δ)-planes at which (4.15) is fulfilled. The dashed curves on the velocity graphs bound the regions of solitary wave existence for the local value of the phase mismatch corresponding to the borders of the regions of solitary waves existence as found by VPS (see their figure 4, (4.7) and the discussion below). The evolution of solitary waves belonging to different families are completely different: the speed of the 'slow' ones tends to the limiting value c_- and their amplitude decreases as the depth diminishes; the amplitude of the 'fast' ones grows very rapidly and their speed becomes close to the local speed of the limiting wave v_+.

To find the dependence of the critical value of the phase mismatch Δ and, hence, of the fluid depth on the initial solitary wave amplitude, numerical calculations were performed in which all solitary waves started from the same initial value of Δ, but had different initial amplitudes. As one could expect the larger the wave, the earlier it reaches the local limiting value of velocity and breaks. The outcome of the calculations was the value Δ_{br} at which this event occurs. Results for two different initial values of phase mismatch are depicted in figure 4.

Although the calculations cannot be continued and the wave evolution traced beyond the dashed lines in figure 3, the physical picture of wave onshore propagation is clear:

the 'slow' waves vanish as their amplitude decreases while the spatial size κ^{-1} tends to infinity as $v \to c_-$;

the 'fast' solitary waves become locally close to the limiting form with a sharp corner at the crest at a certain depth specified by the initial conditions. Further adiabatic evolution is impossible and the waves have no other option but to break.

Note that the effect of inevitable wave breaking in the process of shoaling results

entirely from the resonant interaction of internal waves with the current and has no analogue in the traditional KdV-type theories (see e.g. Grimshaw 1970, 1997; Maslowe & Redekopp 1980), where, as a rule, wave breaking is associated with strong nonlinearity. A peculiar feature of the model derived here is that within the framework of a weakly nonlinear approach it proves to be possible to establish the fact of wave breaking and to specify its conditions.

The range of validity of the employed adiabatic approximation merits a very brief discussion, since this issue was thoroughly studied within the framework of traditional KdV-type models. The bottom slope should be sufficiently mild, so that the wave reflection from the bottom is weak enough to be neglected. Though generation of an oscillatory or aperiodic tail by a shoaling solitary wave does occur and might itself be considered as an important non-adiabatic effect (Johnson 1973; Grimshaw 1979), its influence on the primary wave is negligible to the main order of approximation.

5. Evolution and breaking of shoaling wave: arbitrary bottom slope

Unlike the solitary waves, the periodic ones, in general, have the wavevector k of the order of unity, and therefore the equations (4.9)–(4.11) are strongly interdependent. This means that though non-adiabatic effects due to reflection from the bottom can be neglected for a wave propagating over a gently sloping bottom, the tail or pedestal generated by periodic wave cannot. The effect of the right-hand side of (4.10*b*) is significant and the equations governing the pedestals dynamics do not split from the ones governing the wave part of the solution. The varying pedestal $B(X, T)$, in its turn, affects the wave action and the right-hand side of (4.11) is not negligible, i.e. the wave action is not conserved even in the adiabatic case. Therefore, one has to integrate a system of non-linear PDEs, with the functions to study being related by the integral constraints. The difficulties of obtaining any meaningful results analytically seem to be unsurmountable and the most rational way to proceed is through numerics. However, since the transport equations have already been obtained under certain somewhat restrictive approximations, direct numerical simulation of the initial problem within the framework of the original set (1.1) is a more preferable option. Thus we choose to integrate the system (1.1) directly, which, in particular, enables us to study the non-adiabatic regimes of evolution, i.e. when the scale of the bottom variability is comparable with the scale of nonlinear evolution ($\nu \sim 1$).

The space–time evolution of the periodic initial perturbations was studied with the help of a numeric scheme based on the pseudo-spectral method with respect to spatial variables and the Runge–Kutta method with controlled time-step with respect to the temporal one. The accuracy of the scheme was tested initially for constant Δ by using an exact periodic solution of (3.6) as the initial condition and checking the conservation of two integrals of motion, derived by VPS:

$$\mathscr{P} = \oint \left(a^2 + b^2\right) \mathrm{d}\theta, \tag{5.1a}$$

$$\mathscr{H} = \oint \left(a_x^2 - \Delta a^2 + 2ab - \tfrac{2}{3}b^3\right) \mathrm{d}\theta, \tag{5.1b}$$

in the course of the wave propagation. The first invariant has to be conserved for the case of variable Δ as well and was used to check the validity of the calculations.

The series of simulations was performed for both adiabatically and non-adiabatically sloping depth. In both cases the exact dependence of Δ on the time was taken to be

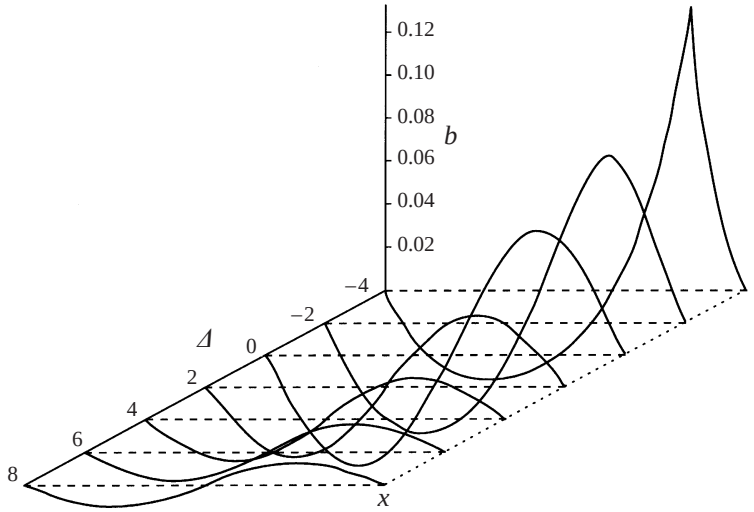

FIGURE 5. Wave evolution up to breaking in the adiabatic case.

a linear function in order to model the most common conditions in the coastal zone. However, as many trial runs revealed, the outcome does not depend noticeably on the functional form of the depth dependence on time as long as its scale is less or comparable to that of nonlinear evolution.

The observed scenarios of wave evolution prove to be very similar and to illustrate the typical adiabatic and non-adiabatic ones we confine ourselves to just two examples. In the first case the function $\Delta = 8 - 0.05t$ was used to model the adiabatic evolution of the wave perturbations; in the second the function $\Delta = 8 - t$ was used. The initial conditions were sinusoidal waves of unitary wavelength and different initial amplitudes, and vorticity and internal wave amplitudes were presumed to be related by (3.2*b*) with $\Delta = 8$. The results of simulations corroborated the qualitative conclusions gained from the adiabatic approach: all waves studied with the initial amplitudes in the range $0.0025 \leqslant b \leqslant 1$ did break within the resonance zone, i.e. at $\Delta > -10$, both in the adiabatic and non-adiabatic case. The principal difference was the nature of the breaking process: in the adiabatic case the waves remained symmetric with respect to the crest up to the formation of the sharp corner at the crest, in full accordance with the expectations. On the other hand, in non-adiabatic case the wave form was more and more distorted as it approached the breaking point, namely the front became much steeper than the rear. Two illustrative examples of the successive change of the wave form for these two cases are shown in figures 5 and 6. In both cases the initial amplitude of the waves was taken to be $b_{in} = 0.01$. In agreement with the theory developed the form of the internal wave perturbation $a(x, t)$ remained smooth up to the moment of breaking.

6. The effect of turbulent viscosity

The starting point of our analysis was the ideal fluid equations (2.1). The particular reason for the neglect of viscous effects is that they are commonly believed to be negligible for motions of the scales under consideration. Yet the specific feature of the motions we describe is the importance for their dynamics of the subsurface layer, where due to wind-wave breaking the turbulence intensity is strongly enhanced and

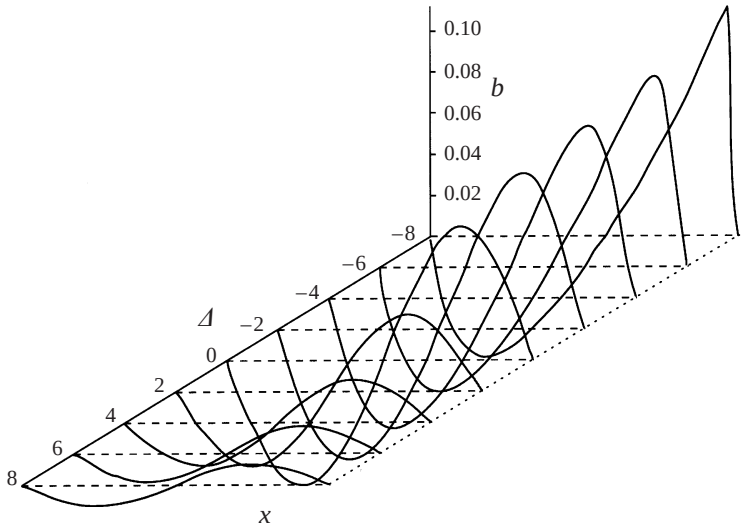

FIGURE 6. Wave evolution up to breaking in the non-adiabatic case.

therefore the values of the viscosity might far exceed those in the main body of the fluid. Thus the question regarding the effect of the turbulence in the subsurface layer on the internal wave–shear flow resonance, raised by a referee, indeed merits a special consideration.

In this section to take the effect of turbulent viscosity into account we start with the full Navier–Stokes equations, i.e. for the horizontal momentum transfer we use (the variables are dimensional)

$$u'_t + (\boldsymbol{u}' \cdot \nabla)u' + \frac{p'_x}{\rho'_0} = \nabla \cdot \left(\nu' \nabla u'\right), \tag{6.1}$$

where $\nu'(z')$ is the turbulent viscosity of the water. Using some suitable value ν_0 as the viscosity scale and employing (2.2) we obtain

$$u_t + (\boldsymbol{u} \cdot \nabla)u + \frac{p_x}{\rho_0} = \eta \left(\nu u_z\right)_z, \tag{6.2}$$

with the horizontal viscous term neglected due to the long-wave approximation adopted. Even if $\nu'(z')$ were of the same order near the surface and in the bulk of the fluid, the coefficient η in the subsurface layer is much greater than in the bulk of the fluid due to the different vertical scales involved, i.e.

$$\eta = \begin{cases} \eta_s = \dfrac{\nu_0 L}{V h^2} & \text{in the subsurface layer,} \\ \\ \eta_b = \dfrac{\nu_0 L}{V H^2} & \text{at depth.} \end{cases} \tag{6.3}$$

Provided the turbulent viscosity is not extremely large, its effect on travelling waves can be taken into account within the framework of the asymptotic approach we have already employed. Namely, suppose that η_s is of order μ. Then $\eta_b \ll O(\mu^5)$, the viscous effects can be safely neglected in the core of the fluid and (2.12) remains intact. In the boundary layer the main-order solution is described by (2.16) again, but

an additional term arises in (2.17):

$$B_\tau - U_\zeta\Big|_{\zeta=0} BB_\chi - \frac{U^2}{U_\zeta}\Big|_{\zeta=0} f_z^{(0)} A_\chi - \frac{\left(\nu U_{\zeta\zeta}\right)_\zeta}{U_\zeta}\Big|_{\zeta=0} B = 0. \tag{6.4}$$

Note that, depending on the particular geometry of the flow, the last term describes damping or amplification of the wave. So far we are not aware of any situations corresponding to wave amplification, although we do not rule out their existence.

By using the scaling transformation (2.18) again we finally obtain a new set of equations instead of (1.1):

$$a_t + \Delta a_x - a_{xxx} - b_x = 0, \tag{6.5a}$$

$$b_t + 2bb_x - a_x + \gamma b = 0, \tag{6.5b}$$

where

$$\gamma = -\left(\nu U_{\zeta\zeta}\right)_\zeta \left(\frac{\alpha\beta^2}{U_\zeta \left(U f_z^{(0)}\right)^6}\right)^{1/4}. \tag{6.5c}$$

The extra term which appears in (6.5*b*) corresponds to the so-called Rayleigh type of damping/pumping, very common in the studies of long-wave dynamics. This is not surprising, as the vertical structure of the Fourier harmonics comprising the long wave is nearly identical and thus the effect of the differential, Navier–Stokes type, friction is the same for all of them. The effect of the Rayleigh friction on the wave is completely different from that of Navier–Stokes friction. Whereas the latter does inhibit higher harmonics, effectively smooths the wave form and, thus, prevents breaking and overturning, the former is only able to provide a certain threshold value for the initial amplitudes, i.e. one would expect the waves of the initial amplitude below the threshold to be dissipated by the friction, but the supercritical ones to develop a sharp corner at the crest and break in spite of the dissipation.

To check this conjecture numerical simulations of (6.5) were performed for different values of the coefficient γ and the initial wave amplitude. The depth dependence in all runs was taken in the form $\Delta = 4 - 0.1t$, which corresponds to a quite mild bottom slope. The results are presented in the figure 7, showing the dependence of the critical initial amplitude of the stationary wave at the depth corresponding to $\Delta = 4$ on the dissipation strength. All waves with amplitudes exceeding the critical one were found to develop a singularity at the crest and eventually break. The results indicate that the viscosity in the subsurface layer has already to be taken into account at values of γ of order of 0.1.

To make a very rough estimate of the viscosity scale corresponding to this value we choose the simplest case of exponential stratification and set the eddy diffusivity to be constant in the boundary layer, i.e. we assume $N = \text{const}$, $\nu = \text{const}$. The estimates based on (6.5*c*) and the equality $\eta_s = \mu$ then are identical and yield

$$\nu_0 = 0.1\,\frac{\pi V h^2}{L}\left(\frac{h}{H}\right)^{1/2}\left|\frac{\left(U_\zeta\right)^{1/4}}{U_{\zeta\zeta\zeta}}\right|_{z=0}. \tag{6.6}$$

We use for quantitative estimates the values of H_0, V, N_0 discussed below in § 7, assuming also $h = 10\,\text{m}$, while (2.6) yields an estimate for the wavelength $L = 1700\,\text{m}$.

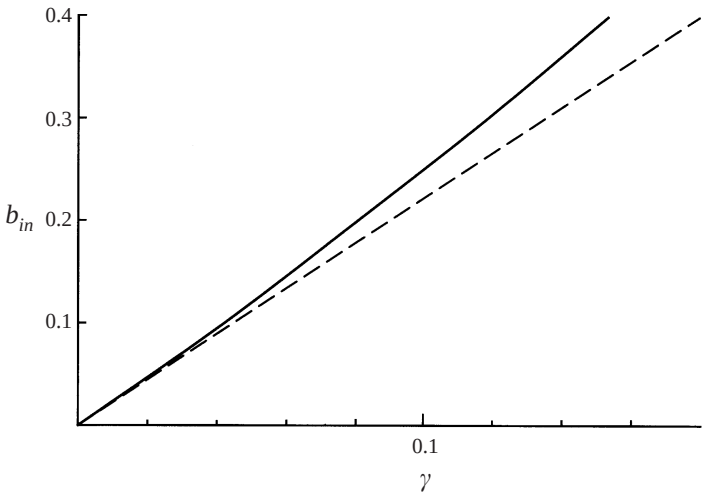

FIGURE 7. Dependence of the critical initial amplitude b_{in} on the dissipation strength γ (solid line). The straight dashed line is given for reference.

The threshold value of the eddy diffusivity then is

$$\nu_0 \approx \left| \frac{(U_\zeta)^{1/4}}{U_{\zeta\zeta\zeta}} \right|_{z=0} \times 5\,\mathrm{cm^2\,s^{-1}}.$$

The main difficulty lies in the fact that not only are the values of the eddy diffusivity beneath the breaking wind waves not well known (for the state of the art knowledge see Terray *et al.* 1996), but also the shear flow geometry near the surface is particularly poorly known. Any judgement on the effect of the viscosity thus strongly depends on a poorly known parameter: the third derivative of the velocity at the surface $U_{\zeta\zeta\zeta}(0)$. Since the nature of the subsurface boundary layer has not been established yet any quantitative estimates would be premature.

7. Concluding remarks

The main conclusion of our analysis is that shoaling internal waves of any small initial amplitude cause breaking in the subsurface layer when passing through the resonance zone. It might be helpful to discuss briefly first the circumstances when these resonance conditions are met and then some immediate implications of the results.

Consider a common situation in which a weak to moderate wind with a speed of, say 5–10 $\mathrm{m\,s^{-1}}$, blows onshore. The wind generates a shear current with velocity at the water surface U_0 of about 3% of the wind speed, i.e around 0.15–0.3 $\mathrm{m\,s^{-1}}$. The phase velocity of long internal waves c_0 strongly depends on both the type and the strength of stratification, which vary widely from place to place and from season to season. However, the simplest rough estimate

$$c_0 \approx \frac{N_0 H}{\pi n}, \tag{7.1}$$

where N_0 is a somehow depth-averaged Brunt–Väisälä frequency, H is the characteristic total depth and n is the vertical mode number, seems to suffice for our purposes.

Setting the current velocity scale to be $\approx 0.2\,\mathrm{m\,s^{-1}}$ and the Brunt–Väisälä frequency N_0 to, say, $10^{-3}\,\mathrm{s^{-1}}$, respectively, the resonance condition $c_0 = U_0$ selects the depth about 600 m for the main mode. For bottom slopes $O(10^{-2})$ or smaller the characteristic width of the resonance zone is 10 km or larger. Moreover, there is a sequence of such zones corresponding to the resonances with the first few higher vertical modes of internal waves, since the higher modes reach resonance at roughly n-times larger depths. For situations characterized by very sharp pychnoclynes, such higher-mode zones might be absent, since the level of higher modes is quite low, while for the main mode (7.1) underestimates the phase velocity c_0 and thus the first resonance zone can be shifted somewhat closer to the shore.

To quantify the contribution to mixing of the mechanism considered one should, apart from specifying the statistics of the incoming internal wave field, details of stratification and shear profiles, investigate in more detail the breaking itself, which goes beyond the scope of the present study. However, it is worth mentioning that in our view in contrast to the studies of gravity internal wave breaking (see e.g. Michallet & Ivey 1999), the main role of the breaking events in the subsurface layer we studied is in triggering more intense breaking of wind waves. Indeed, a breaking event in the subsurface layer should result in its local widening and a drop of current velocity at the surface. The wind waves, being extremely sensitive to even the smallest non-uniformity of the shear current, increase locally their intensity of breaking and thus further enhance the local anomaly of the shear current. The manifestations of such a scenario are expected to be observable even by an unaided eye as wide streaks of more intense wind-wave breaking parallel to the shoreline. The streaks can be also detected from satellites both in the visual range as lines of higher albedo, and in the microwave and infrared ranges as a sea surface anomaly. Direct *in situ* experimental verification of the suggested picture by existing technical means is hardly feasible in the foreseeable future because of the necessity to carry out high accuracy current measurements in the subsurface layer in the presence of quite intense wind waves. At present the only ways open are accumulation of indirect evidence and developing new remote sensing techniques able to discern these processes. A realistic much more feasible first step would be direct experimental testing of the described scenarios in laboratory conditions; we see no serious obstacles to this.

It is worth mentioning that although our prime motivation in this work was to investigate the dynamics of the uppermost ocean layer, the derived model is equally applicable for describing the resonance between internal waves and the bottom boundary layer current. The processess resulting in enhancing of mixing in the vicinity of the bottom are of special interest in the context of sediment transport.

V. V. V. wishes to thank V. Geogjaev for helpful discussions. The authors also thank an anonymous referee for the helpful comments.

The work was supported by Forbairt Basic Research Grant SC-98-530, by INTAS (Grant 97-575) and by Russian Foundation for Basic Research (Grant 97-05-65070).

REFERENCES

Agnon, Y., Pelinovsky, E. N. & Sheremet, A. 1998 Disintegration of cnoidal waves over smooth topography. *Stud. Appl. Maths* **101**, 49–71.

Akylas, T. R. & Benney, D. J. 1980 Direct resonance in nonlinear wave systems. *Stud. Appl. Maths* **63**, 209–226.

Bretherton, F. P. & Garrett, C. J. R. 1968 Wavetrains in inhomogeneous moving media. *Proc. R. Soc. Lond.* A **302**, 539–554.

Camassa, R. & Holm, D. D. 1993 An integrable shallow water equation with peaked solitons. *Phys. Rev. Lett*. **71**, 1661–1664.

Case, K. M. 1960 Stability of inviscid plane Couette flow. *Phys. Fluids* **3**, 143–148.

Dickey, L. A. 1960 Stability of plane-parallel flows of an ideal fluid. *Dokl. Acad. Sci. USSR* **125**, 1068–1071.

Fornberg, B. & Whitham, G. B. 1978 A numerical and theoretical study of certain nonlinear wave phenomena. *Phil. Trans. R. Soc. Lond.* A **289**, 373–404.

Friedland, L. 1998 Autoresonance of coupled nonlinear waves *Phys. Rev.* E **58**, 3494–3501.

Gear, J. A. & Grimshaw, R. 1984 Weak and strong interactions between internal solitary waves. *Stud. Appl. Maths* **70**, 235–258.

Grimshaw, R. H. J. 1970 The solitary waves in water of variable depth. I. *J. Fluid Mech.* **42**, 639–656.

Grimshaw, R. H. J. 1979 Slowly varying solitary waves. 1. Korteweg – de Vries equation. *Proc. R. Soc. Lond*. A **368**, 359–375.

Grimshaw, R. H. J. 1997 Internal solitary waves. In *Advances in Coastal and Ocean Engineering* (ed. P. L.-F. Liu), vol. 3, pp. 1–30. World Scientific.

Grimshaw, R. H. J. 2000 Models for long-wave instability due to a resonance between two waves. In *Trends in Applications of Mathematics to Mechanics* (ed. G. Iooss, O. Gues & A. Nouri), pp. 183–192. Chapman & Hall/CRC.

Johnson, R. S. 1973 On an asymptotic solution of the Korteweg – de Vries equation with slowly varying coefficients. *J. Fluid Mech.* **60**, 813–824.

LeBlond, P. H. & Mysak, L. A. 1979 *Waves in the Ocean*. Elsevier.

Maslowe, S. A. & Redekopp, L. G. 1980 Long nonlinear waves in stratified shear flows. *J. Fluid Mech.* **101**, 321–348.

Michallet, H. & Ivey, G. N. 1999 Experiments on mixing due to internal solitary waves breaking on uniform slope. *J. Geophys. Res.* **104C**, 13467–13477.

Ostrovsky, L. A. & Pelinovsky, E. N. 1975 Refraction of nonlinear sea waves in the coastal zone. *Izv., Atmos. Ocean. Phys.* **11**, 37–41.

Pelinovsky, E. N. 1996 *Tsunami Waves Hydrodynamics*. Institute of Applied Physics, Nizhny Novgorod.

Peregrine, D. H. & Thomas, G. 1979 Finite-amplitude deep-water waves on currents. *Phil. Trans. R. Soc. Lond*. A **292**, 371–390.

Reutov, V. P. 1990 On the instability of internal wave in a stratified fluid with shear flow near the surface. *Izv., Atmos. Ocean. Phys.* **26**, 638–642.

Shrira, V. I. 1989 On the 'sub-surface' waves of the mixed layer of the upper ocean. *Dokl. Akad. Nauk SSSR* **308**, 732–736. English translation: *Trans. USSR Acad. Sci., Earth Sci. Sec.* **308**, 276–279.

Terray, E. A., Donelan, M. A., Agrawal, Y. C., Drennan, W. M., Kahma, K. K., Williams, A. J., Hwang, P. A. & Kitaigorodski, S. A. 1996 Estimates of kinetic energy dissipatrion under breaking waves. *J. Phys. Oceanogr*. **26**, 792–807.

Voronovich, V. V., Pelinovsky, D. E. & Shrira, V. I. 1998 On internal wave–shear flow resonance in shallow water. *J. Fluid Mech.* **354**, 209–237 (referred to herein as VPS).

Voronovich, V. V. & Shrira, V. I. 1996 On the amplification of internal-wave surface manifestations due to subsurface shear current. *Oceanology* **36**, 157–161.

Voronovich, V. V., Shrira, V. I. & Stepanyants, Yu. A. 1998 Two-dimensional models for nonlinear vorticity waves in shear flows. *Stud. Appl. Maths* **100**, 1–32.

Whitham, G. B. 1965 A general approach to linear and nonlinear water waves using a Lagrangian. *J. Fluid Mech.* **22**, 273–283.

Whitham, G. B. 1974 *Linear and Nonlinear Waves*. John Wiley & Sons.